

⁶Raman, G., Rice, E. J., and Cornelius, D., "Evaluation of Flip-Flop Jet Nozzles for Use as Practical Excitation Devices," *Journal of Fluids Engineering, Transactions of the ASME*, Vol. 116, 1994, pp. 508-515.

⁷Raman, G., and Rice, E. J., "Development of Phased Twin Flip-Flop Jets," *Journal of Vibration and Acoustics, Transactions of the ASME*, Vol. 116, 1994, pp. 263-268.

⁸Davis, M. R., "Variable Control of Jet Decay," *AIAA Journal*, Vol. 20, No. 5, 1982, pp. 606-609.

⁹Brown, W. H., and Ahuja, K. K., "Jet Mixing Enhancement by Hydrodynamic Excitation," *AIAA Paper 90-4005*, 1990.

¹⁰Lepicovsky, J., and Brown, W. H., "Effects of Nozzle Exit Boundary Layer Conditions on Excitability of Heated Jets," *AIAA Journal*, Vol. 27, 1989, pp. 712-718.

¹¹Moffat, R. J., "Using Uncertainty Analysis in the Planning of an Experiment," *Journal of Fluids Engineering, Transactions of the ASME*, Vol. 114, 1985, pp. 362-366.

Turbulent Manipulation of Condensation at a Shock Tube's Contact Surface

Upul De Silva,* Aric Gardner,[†]
and

Joseph A. Johnson III[‡]

Florida Agricultural and Mechanical University,
Tallahassee, Florida 32310

Introduction

AN improved understanding of condensation phenomena in gaseous flow would have tremendous application to technological and scientific problems including droplet induced erosion in turbine blades, production of undesirable environmental conditions due to the condensation trails left by jet engines, and the inhibition of combustion in combustors. The usefulness of the shock tube for condensation studies was established by Wegener and Lundquist¹ followed by Glass and Patterson,² Barschdorff,³ Sislian and Glass,⁴ Kotake and Glass,⁵ and Glass et al.⁶ The development of the theory of nucleation rate and growth rate of the clusters is elaborated in the work of Lothe and Pound,^{7,8} Dunning,⁹ Wegener,¹⁰ and Refs. 11-15. In recent experiments carried out by Britan et al.,¹⁶ the effects of condensation on the parameters of the flow behind shock waves in water vapor were investigated in detail. Another recent experiment conducted by Schnerr and Bohning¹⁷ investigated the effects of the heat addition by homogenous condensation on the compressible turbulent boundary layer. Nonetheless, in spite of all of this work, the relationship between the governing thermodynamic parameters and the simplest parameters in nucleation (such as onset and droplet growth rate) is not well understood at all.

It is particularly clear that no experimental treatment has determined either the role which turbulence plays in the observations, if any, or the implications for such a possible role in the development of a reliable physical model. Implicitly, all current theories for droplet sizes also assume no role for turbulence. We, therefore, examine in this paper the possibility of a relationship between condensation and turbulence using the reliable and predictable turbulent environment of a shock tube's contact surface as a test system for water vapor condensation. We do not concern ourselves, at this juncture, with the onset of condensation. Our main interest is to investigate experimentally the effect that turbulence has on an existing condensation front which is moving with the turbulent gaseous media.

Experimental Facilities and Test Conditions

A pressure driven shock tube (Fig. 1) consisting of a driver section of 60×5.2 in., a driven section with a test section of 60×5.2 in., and an extension tube of 76×5.2 in. was used to carry out the experiment. Aluminized Mylar[®] sheets of various thicknesses were used as the material for the diaphragm which separates the driver section from the driven section. The compressed air is supplied to the driver section from a reservoir where the relative humidity of the air could be controlled by controlling the temperature in the driver gas. A heating tape is wrapped around (outside) the entire driver section, and a thermocouple probe is used in the driver section to measure the initial temperature.

The test section has three stations for optical diagnostics, two of which consist of four perpendicular glass ports; the other station has two inline glass ports. The test section is also equipped with several ports for pressure transducers. A 50-mW He-Ne laser is used for right-angle scattering through the optical station which is 2.5 ft downstream of the diaphragm. Two pressure transducers are mounted on either side of the optical station, 2 ft apart; pressure histories along with histories of the scattered signal at right angles are recorded on a four-channel 500-MHz Tektronix digital oscilloscope. All of the signals are stored on floppy disks. The optics for receiving the scattered signal from the droplets (Fig. 1b, no. 3) included a neutral density filter; the received signals are transmitted to the photomultiplier tubes using fiber optics and also stored on the oscilloscope just mentioned.

It has already been shown that in a pressure driven shock tube at a shock wave velocity of $M = 1.8$ the contact surface is fully turbulent.¹⁸ A TSI three-dimensional laser doppler velocimeter (LDV) system is used to confirm the existence of turbulence in all three components of the local velocity at the contact surface; it consists of a 6-W Ar-ion laser, a color separator, a color link (photo multiplier tubes and amplifiers), a burst correlator (signal processor) and a 486 computer controller. For seeding the flow, $0.8\text{-}\mu\text{m}$ latex particles and incense smoke were used on both driver and driven sections. The overall data rate for the LDV during the approximately 500 μs of turbulent flow (all components) exceeded 30 kHz. Fourier analysis of the velocity fluctuations (all components) showed turbulent fluctuation spectra and turbulent autocorrelation profiles consistent with the results previously reported on density fluctuations in Ref. 18. The typical turbulent environment

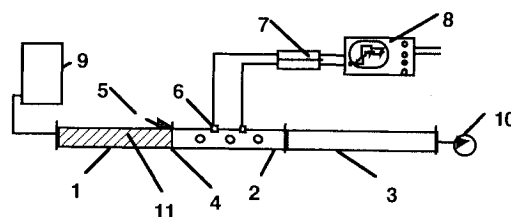


Fig. 1a Shock tube schematic: 1) driver section, 2) test section, 3) extension tube, 4) position of diaphragm, 5) plunger, 6) quartz pressure transducers, 7) signal amplifiers, 8) digitizing oscilloscope, 9) high-pressure tank, 10) vacuum pump, and 11) heating tape.

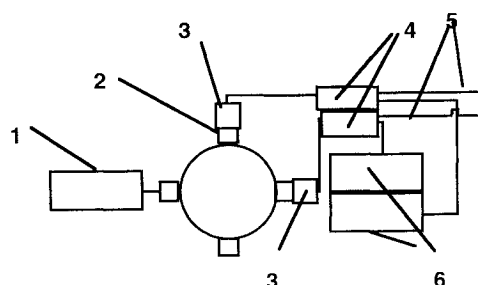


Fig. 1b Cross section of optical station showing right-angle scattering system (LDV setup not shown): 1) 50-mW He-Ne laser, 2) optical ports of the test section, 3) receiving optics, 4) phase modulated transmitter, 5) cables to oscilloscope, and 6) high-voltage power supplies.

Received Feb. 25, 1994; revision received Oct. 19, 1994; accepted for publication Oct. 19, 1994. Copyright © 1994 by the American Institute of Aeronautics and Astronautics, Inc. All rights reserved.

*Graduate Research Assistant, Department of Mechanical Engineering, College of Engineering, Student Member AIAA.

[†]Undergraduate Research Assistant, Department of Physics.

[‡]Distinguished Professor of Science and Engineering, Associate Fellow AIAA.

at the contact surface showed rms velocity fluctuations in all three components at approximately 33% the local speed of sound.

The characteristic relationship between a turbulent intensity sensitivity parameter and the local Reynolds number for fully developed turbulence with a dominant mode has been suggested by previous theoretical work^{19,20}; evidence supporting this behavior has already been found in detonation waves²¹ and in reacting turbulent polymers.²² We speculate, for our purposes in this paper, that the sizes of the droplets might be sensitive to changes in the turbulent intensity and, therefore, sensitive to changes in Reynolds number.

The experimental conditions are determined from trial firings at increasing relative humidity in the supply driver gas (compressed air) at room temperature until the scattered signal from the droplets is found to be coincident with the contact surface. We have thereby determined that, at an appropriate relative humidity (roughly 60% at Standard temperature and pressure), a condensation front can be produced in the supersaturated driver gas so as to be coincident with the contact surface. The relative humidity in the supply gas is then fixed throughout the entire series of subsequent firings. The shock wave velocity is also fixed at $M = 1.8$ by fixing the pressure ratio P_4/P_1 . Shock wave Mach number M_S (and therefore the contact surface velocity) were very strictly controlled. For each run the velocity of the shock wave was measured using the quartz pressure transducers; data obtained from runs with even a slightly different flow velocity due, e.g., to uneven ruptures of the diaphragm, were ignored. At this Mach number and, consequently, at a fixed contact surface velocity, we change P_4 (at constant P_4/P_1) and thereby change the Reynolds number Re of the flow. Thus, for the same flow velocity, we record the scattered and attenuated signals from water droplets for different values for Re . Subsequently, the same series of firings is repeated at an increased initial temperature and then an even higher initial temperature. P_4 (initial pressure of the high-pressure side) and P_1 (initial pressure of the low-pressure side) were varied between 27–63.5 psia and 1.4–3.5 psia, respectively. In addition, all run conditions were repeated at least twice so as to determine the reliability of the light scattering results.

The velocity of the contact surface was calculated from the standard one-dimensional shock tube relationships²³ after the shock wave velocity has been measured; this calculation was confirmed by the LDV measurements, the agreement between the two determinations thereby confirming the applicability of the one-dimensional relationships for the system. The scattered laser light signal and the simultaneous attenuated light signal were converted to particle sizes by using Rayleigh's scattering theory^{24–26}; for convenience, all scattering droplet sizes are normalized to the first measured droplet size (which we determined using standard techniques described in the cited references to be roughly 0.265μ) at the initial Re . The percentages of the change of size of particles with respect to the initial size of the particles were calculated for different Re and different temperature levels.

Results and Discussion

The results are shown in Fig. 2. The measured relationships between the percentage of relative particle size changes and Reynolds number at the contact surface are given. The Reynolds numbers for conditions at the contact surface were calculated assuming one-dimensional flow and using values for dynamic viscosity taken from the standard tables.²⁷ Figure 2 shows that the droplet sizes increase, at fixed Re , with decreasing temperature in a manner consistent with current theoretical consensus (as elaborated in Ref. 24). Figure 2 also shows, independent of temperature, a pronounced dependence of droplet size on Reynolds number. Specifically, after a regime of increasing droplet size with Reynolds number and a sensitivity to turbulence, the turbulence sensitivity is saturated and the further increases in Reynolds number provide an associated slow decrease in droplet size. This means that, for each system, a maximum droplet size can be reached, insofar as the influence of turbulence is concerned, beyond which (as the Reynolds number increases) the influence of turbulence will not be particularly important.

The nature of the dependence of a turbulent intensity dependent parameter on Reynolds number for turbulent systems characterized by dominant modes (and an associated characteristic frequency)

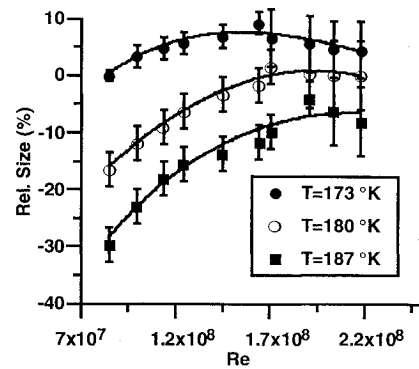


Fig. 2 Evidence of influence of turbulence on condensation: percentage change in droplet size (compared to size at lowest Reynolds number and lowest temperature) plotted vs Reynolds number at the contact surface $Re_3 = \rho_3 U_3 D / \mu_3$ where μ is dynamic viscosity,²⁷ ρ density calculated from the equation of state, U velocity of the flow, and D the inner diameter of the tube. Temperature $T (= T_3)$ is calculated using the equations for one-dimensional flow in the shock tube's expansion fan and measured values of local static pressure. Errors determined from repeated measurements at the same run conditions.

is discussed in detail in Ref. 20. This dependence as originally derived by Tsugé¹⁹ is standard for the Orr-Sommerfeld class of equations. That is, for each characteristic frequency, there is 1) an onset Reynolds number followed by a regime in which increasing turbulent intensities are associated with increasing Reynolds numbers; 2) a regime (brief) during which the turbulent intensity is not very sensitive to Reynolds numbers, identified by a Reynolds number of peak turbulent intensity (the peak Reynolds number); followed by 3) a regime during which the increasing Reynolds numbers are associated with decreasing turbulent intensities. As the value of the peak Reynolds number increases, for each characteristic frequency, the rate of change of turbulent intensity with Reynolds number, in regime 1, also increases and the separation between regimes 1 and 3 is more precisely defined.

Figure 2 shows that the Tsugé behavior is suggested for the influence of turbulence on condensation. We consider the implicit extrapolation of the fitted curves to both lower and higher Reynolds numbers in the context of Ref. 20. As the peak Reynolds numbers increase, the importance of turbulence to condensation processes is restricted to an increasingly narrow range of Reynolds numbers with an increasingly large dynamic range in the ratio of droplet sizes. If, however, turbulence is associated with low-peak Reynolds number flow, the sizes of the droplets in the condensation are quite sensitive indeed to Reynolds number, and a manipulation of the Reynolds number can provide a corresponding manipulation of the droplet sizes.

Acknowledgment

This work was supported in part by NASA Grant NAGW-2930 to Florida Agricultural and Mechanical University.

References

- Wegener, P., and Lundquist, G., "Condensation of Water Vapor in the Shock Tube Below 150°K," *Journal of Applied Physics*, Vol. 22, Feb. 1951, p. 233.
- Glass, I. I., and Patterson, G., "A Theoretical and Experimental Study of Shock Tube Flows," *Journal of Aeronautical Science*, Vol. 22, Feb. 1977, pp. 73–100.
- Barschdorff, D., "Carrier Gas Effects on Homogeneous Nucleation of Water Vapor in a Shock Tube," *Physics of Fluids*, Vol. 18, May 1975, pp. 529–535.
- Sislian, J. P., and Glass, I. I., "Condensation of Water Vapor in Rarefaction Waves: I. Homogeneous Nucleation," *AIAA Journal*, Vol. 14, No. 12, 1976, pp. 1731–1737.
- Kotake, S., and Glass, I. I., "Condensation of Water Vapor in Rarefaction Waves: II. Heterogeneous Nucleation," *AIAA Journal*, Vol. 15, No. 2, 1977, pp. 215–221.
- Glass, I. I., Kalra, S. P., and Sislian, J. P., "Condensation of Water Vapor in Rarefaction Waves: III. Experimental Results," *AIAA Journal*, Vol. 15, No. 5, 1977, pp. 686–693.
- Lothe, J., and Pound, G. M., "Reconsiderations of Nucleation Theory," *Journal of Chemical Physics*, Vol. 36, No. 8, 1962, pp. 2080–2085.

⁸Lothe, J., and Pound, G. M., "Statistical Mechanics of Nucleation," *Nucleation*, edited by A. C. Zettlemoyer, Marcel Dekker, New York, 1969, Chap. 3.

⁹Dunning, W. J., "General and Theoretical Introduction," *Nucleation*, edited by A. C. Zettlemoyer, Marcel Dekker, New York, 1969, Chap. 1.

¹⁰Wegener, P. P., "Gas Dynamics of Expansion Flows with Condensation and Homogeneous Nucleation of Water Vapor," *Nonequilibrium Flows*, Pt. 1, Vol. 1, edited by P. P. Wegener, Marcel Dekker, New York, 1970, Chap. 4.

¹¹Wegener, P. P., and Pouring, A. A., "Experiments on Condensation of Water Vapor by Homogeneous Nucleation in Nozzles," *Physics of Fluids*, Vol. 7, No. 3, 1964, pp. 352-361.

¹²Wegener, P. P., Clumpner, J. A., and Wu, B. J. C., "Homogeneous Nucleation and Growth of Ethanol Drops in Supersonic Flow," *Physics of Fluids*, Vol. 15, Nov. 1972, pp. 1869-1876.

¹³Wegener, P. P., and Mack, L. M., "Condensation in Supersonic and Hypersonic Wind Tunnels," *Advances in Applied Mechanics*, Vol. 5, edited by H. L. Dryden and T. von Kármán, Academic, New York, 1958, pp. 307-447.

¹⁴Wegener, P. P., "Nucleation of Nitrogen: Experiment and Theory," *Journal of Physical Chemistry*, Vol. 91, No. 10, 1987, pp. 2479-2481.

¹⁵Wu, B. C., Wegener, P. P., and Stein, G. D., "Homogeneous Nucleation of Argon Carried in Helium in Supersonic Nozzle Flow," *Journal of Chemical Physics*, Vol. 69, No. 4, 1978, pp. 1776-1777.

¹⁶Britan, A. B., Zuev, A. P., and Khmelevskii, A. N., "The Effect of Condensation on the Parameters of the Flow behind Shock Waves in Water Vapor," *Zhurnal Tekhnicheskoi Fiziki*, Vol. 62, July 1992, pp. 765-770.

¹⁷Schnerr, G. H., and Bohning, R., "Compressible Turbulent Boundary Layers with Heat Addition by Homogeneous Condensation," *AIAA Journal*, Vol. 30, No. 5, 1992, pp. 1284-1289.

¹⁸Johnson, J. A., III, Santiago, J., and Jones, W. R., "Driver Gas Flow with Fluctuations," *Journal of Physics D: Applied Physics*, Vol. 13, 1980, pp. 1413-1425.

¹⁹Tsugé, S., "Approach to the Origin of Turbulence on the Basis of Two-Point Kinetic Theory," *Physics of Fluids*, Vol. 17, Jan. 1974, pp. 22-33.

²⁰Johnson, J. A., III, and Ramaiah, R. I. L., "Reduced Molecular Chaos and Flow Instability," *Stability in the Mechanics of Continua*, edited by F. H. Schroeder, Springer-Verlag, Berlin, 1982, pp. 318-329.

²¹Johnson, J. A., III, "A Boundary-Layer Treatment for Turbulent Detonation Waves," *Applied Physics Letters*, Vol. 37, No. 3, 1980, pp. 275-276.

²²Johnson, J. A., III, and Santiago, J., "Turbulent Boundary Layer Treatment for Reacting Polymer Jets," *Polymer Communications*, Vol. 25, Feb. 1984, pp. 34, 35.

²³Gaydon, I. G., and Hurle, I. R., *The Shock Tube in High Temperature Physics and Chemistry*, Reinhold, New York, 1963, pp. 1-23.

²⁴Stein, G. D., and Wegener, P. P., "Experiments on the Number of Particles Formed by Homogeneous Nucleation in the Vapor Phase," *Journal of Chemical Physics*, Vol. 46, 1967, pp. 3685, 3686.

²⁵Kerker, M., *The Scattering of Light*, Academic Press, New York, 1969, Chap. 3.

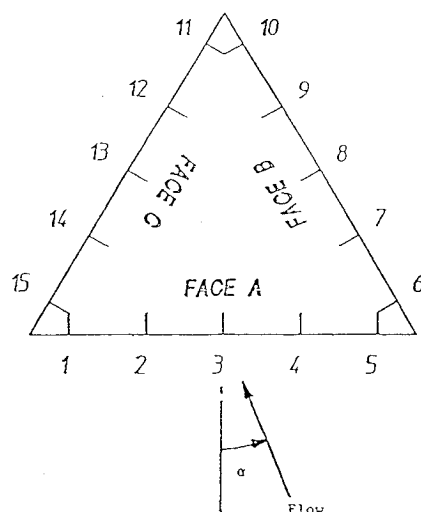
²⁶Shirinzadeh, B., Hillard, M. E., and Exton, R. J., "Condensation Effects on Rayleigh Scattering Measurements in a Supersonic Wind Tunnel," *AIAA Journal*, Vol. 29, No. 2, 1991, pp. 242-246.

²⁷Keenan, J. H., Chao, J., and Kaye, J., *Gas Tables—Thermodynamic Properties of Air, Products of Combustion and Component Gases, Compressible Flow Functions*, 2nd Ed., Wiley, New York, 1980.

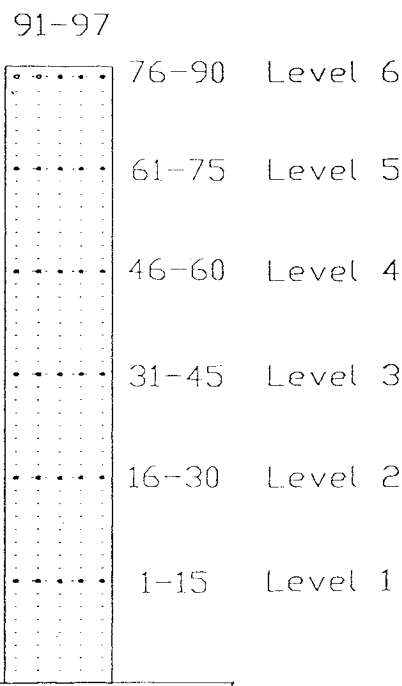
end of the prism. It is thus desirable to know the extent of the wind loads variation at the free end of a prism due to changes in the incident turbulence characteristics of the natural wind for realistic wind-tunnel model tests. Flow patterns and pressure distributions around triangular prisms in smooth, uniform, two-dimensional flow without end effects were previously studied by El-Sherbiny¹ and Twigge-Molecey and Baines.² For finite length triangular prisms, however, no study on the effects of turbulence intensities on the surface pressures of the prisms has been cited in the literature. Finite length triangular prisms are now regularly being used as the main structural members of offshore oil rigs, telecommunication towers, etc. Some high-rise buildings are also of triangular shape.

Experiment, Results, and Discussion

The model (Fig. 1) used is an equilateral triangular prism with constant cross section. The width d of each side of the prism is 100 mm with an aspect ratio of 6. The prism was tested in the freestream of the wind tunnel without turbulence grid (turbulent intensity, $k \cong 0.5\%$) and with two different turbulence grids ($k \cong 10$ and 30%). There are 97 pressure tapping points Fig. 1(b) on the prism. The distance between each level of the circumferential



a)



b)

Effects of Free End and Turbulence Intensities on Triangular Prism

T. S. Lee*

National University of Singapore, 0511 Singapore

Introduction

FOR three-dimensional prisms of finite length in natural wind environments, the influx of fluid from the top end of the prism can cause considerable alterations to the vortex-shedding process near the free end and hence variation of the loadings over the top

Received July 10, 1993; revision received March 21, 1994; accepted for publication March 23, 1994. Copyright © 1994 by the American Institute of Aeronautics and Astronautics, Inc. All rights reserved.

*Mechanical and Production Engineering Department.

Fig. 1 Pressure tapping locations: a) plan view: level 1 and b) elevations: levels 1-6.